Visible Upconversion Luminescence from Y 2 O 3 :Eu 3+ ,Yb 3+

ARTICLE *in* THE JOURNAL OF PHYSICAL CHEMISTRY C · OCTOBER 2008

Impact Factor: 4.77

Visible Upconversion Luminescence from Y_2O_3:Eu^{3+},Yb^{3+}

Huaishan Wang, Chang-kui Duan, and Peter A. Tanner*

Department of Biology and Chemistry, City University of Hong Kong, Tat Chee Avenue, Kowloon. Hong Kong

Received: May 27, 2008

A red upconverted emission is reported for yttria codoped with Eu^{3+} and Yb^{3+} upon excitation by a 970 nm laser diode. The concentration dependence and temperature dependence down to 10 K of the upconverted emission have been investigated. Two alternative models are presented to simulate the emission intensity−temperature dependence.

1. Introduction

Producing visible photons from infrared (IR) ones by upconversion in solid-state systems has been an active field of research in recent years and has been reviewed by several authors.[1−3] The diverse applications of upconversion lie in the fields of display devices, lasers, radiation detectors, and biolabels. Most of the systems investigated involve two-body processes involving transfer from the donor sensitizer to an excited state of the activator ion. Systems with 5- and 6- photon upconversion have been reported.[4] The Yb^{3+} ion has strong absorption bands near 1 μm and has frequently been used as a dopant ion to sensitize visible emission, in particular for Er^{3+} as an activator.[5−7] The criteria desirable for the host lattice include good thermal and hardness properties, optical transparency, low vibrational frequencies, and short donor−acceptor distances. Nevertheless, fluoride and oxide hosts with higher vibrational quanta have frequently been employed, rather than chloride or bromide host lattices, because of their superior chemical inertness and durability. Upconversion involving three bodies is generally 1 or 2 orders of magnitude less efficient than two-body processes and has been less-studied. Auzel first proposed and investigated the stepwise upconversion process.[8,9] Miyakawa and Dexter formulated the mechanisms for cooperative and stepwise upconversion and pointed out that the dominance of the cooperative process will only occur when the acceptor ion has no available intermediate state near to that of the donor ion.[10] The importance of three body processes in energy transfer was subsequently emphasized by Fong and Diestler[11] and Kushida.[12] Some new three-body processes, including phonon-assisted three-body transfer and second-order cooperative transfer, were proposed by Chua and Tanner.[13] More recently, Güdel and co-workers have proposed exchange-coupled dimer systems to explain the energy transfers between Yb^{3+} and Tb^{3+},[14,15] and Yb^{3+} and Mn^{2+}.[16,17]

The most popular lanthanide (Ln^{3+}) ion in phosphors for red emission is Eu^{3+}, with $^5D_0 \rightarrow {}^7F_1$, $^7F_2$ bands near 600 nm. The spectra of Eu^{3+}[18] and of Yb^{3+}[19] in the Y_2O_3 host have previously been investigated, but we are unaware of any previous studies of the codoped system. Previous studies of Yb^{3+}−Eu^{3+} upconversion have utilized oxyfluoroborate glass,[20] silica glass,[21] and $Li_2Lu_5O_4(BO_3)_3$.[22] In this study, we have employed the host lattice Y_2O_3 to investigate the upconversion from Yb^{3+} to Eu^{3+}. The reverse-energy transfer process was investigated in the 1970s by Yamada et al.[23] and attributed to a dipole−quadrupole energy-transfer mechanism. More recently, Yuan et al. have formulated the charge transfer mechanism, in addition to the cooperative transfer mechanism, for the downconversion in Y_2O_3:Yb^{3+},Tb^{3+}.[24]

The relevant energy levels of Eu^{3+} and Yb^{3+} to this study have previously been assigned.[18,19,25] There are some alternative assignments in the literature for the $^2F_{5/2}$ and $^2F_{7/2}$ crystal-field levels of Yb^{3+} in Y_2O_3. These most likely arise because of the presence of electron−phonon coupled states, as observed and assigned for some other Yb^{3+} systems.[26] For example, there are two absorption bands at ∼10 684 and 10 504 cm^{-1} for Yb_2O_3, whereas the relevant calculated energy level is 10629 cm^{-1}. Because the lowest $^2F_{5/2}$ state is at 10 225 cm^{-1}, resonance of an electronic state (located at the energy near to the calculated value) with the Raman 379 cm^{-1} phonon[19] excited in the lowest level could lead to two vibronic states.

2. Experimental Section

Y_2O_3:Eu^{3+},Yb^{3+} samples with various doping concentrations were prepared by a sol-lyophilisation process,[27,28] followed by calcination at 1000 °C for two hours. In brief, yttrium, ytterbium, and europium nitrates were obtained from their oxides by dissolution in nitric acid, and the addition of NaOH under continuous stirring gave a precipitate, which was washed under ultrasonication, centrifuged, and dispersed in water. The so-obtained sol was freeze-dried at −10 °C and dried at 130 °C. The powder obtained was then thermally annealed at 1000 °C. All chemicals: Y_2O_3 (5N, Strem Chemicals), Eu_2O_3 (5N, Sigma-Aldrich), and Yb_2O_3 (4N, International Laboratory USA and 5N, American Elements, USA) were used as received without further purification.

Powder X-ray diffraction was carried out on a Siemens D501 diffractometer with Cu Kα_1 radiation produced at 40 kV. The diffraction pattern was acquired over the range of 10 to 80° in steps of 0.04° and the accumulating time of 1 s per step. All systems were cubic and according to the Scherrer formula, and the average size of the crystallites was calculated to be around 30 nm for most of the obtained powders, with some XRD patterns shown in Figure 1. The diffuse reflectance spectra were recorded by a PerkinElmer Lambda 750 wide-range spectrophotometer. Photoluminescence spectra were recorded using a Spectrapro 500i monochromator from Acton Research with a 970 nm laser diode as excitation source. The detection was by a Hamamatsu R928 photomultiplier tube. Although most experiments were performed at room temperature, the temper-

* To whom correspondence should be addressed. E-mail: bhtan@cityu.edu.hk. Tel: +852 2788 7840. Fax: +852 2788 7406.

10.1021/jp8046505 CCC: $40.75
Published on Web 09/25/2008

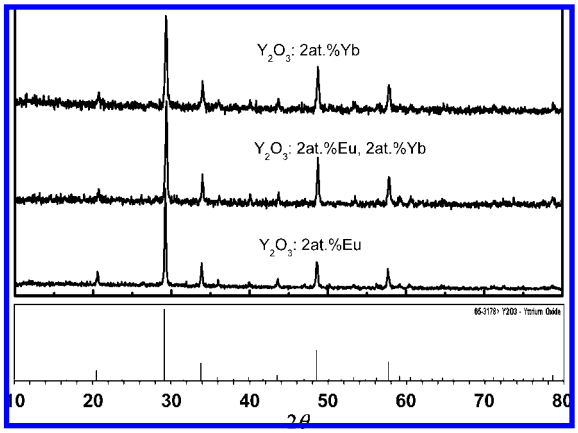

Figure 1. XRD patterns of the calcined powder samples with different doping concentration as well as JCPDS card 65−3178 for Y_2O_3. The ordinate is intensity in arbitrary units.

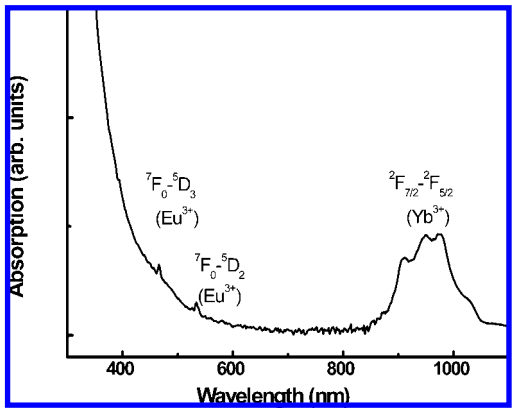

Figure 2. Room-temperature near-IR and visible diffuse reflectance spectrum of Y_2O_3: 1 atom % Eu^{3+}, 2 atom % Yb^{3+}.

ature dependence of the upconversion was determined by housing the sample in an Oxford Instruments closed-cycle cryostat with base temperature ~10 K.

3. Results

Figure 2 shows the room temperature diffuse reflectance spectrum of Y_2O_3:Yb^{3+},Eu^{3+}. The strongest absorption is due to the $^2F_{7/2} \rightarrow {}^2F_{5/2}$ transition of Yb^{3+}, assigned previously by Laversenne et al.,[19] whereas the Eu^{3+} absorption bands are much weaker. The 970 nm diode laser is thus suitable for excitation of Yb^{3+}, and the room temperature emission spectrum of Y_2O_3:Yb^{3+} using this excitation source is shown in Figure 3. The intense bands near 550 and 650 nm are due to a trace impurity of Er^{3+} present in the 4N Yb_2O_3. These bands persisted in our experiments using double-doped systems although they were less intense when using 5N Yb_2O_3 starting material. The bands above 500 nm are due to the cooperative upconversion of Yb^{3+} ions and are similar to the spectrum reported for $(Yb_{0.05}Y_{0.95-x}La_x)_2O_3$ ceramics.[29] The Yb^{3+} cooperative emission has also been studied in other systems.[30]

Red emission was observed from double-activated Y_2O_3:Eu^{3+},Yb^{3+} upon 970 nm excitation (Figure 4). The emission bands shown are clearly assigned to the $^5D_0 \rightarrow {}^7F_J$ ($J = 0, 1, 2$) transitions of Eu^{3+}.[25] The upconversion emission was not obtained for single-doped Y_2O_3:Eu^{3+} because there is a considerable mismatch with Eu^{3+} energy levels when using the excitation at 970 nm (~10 300 cm^{-1}). On codoping the Y_2O_3:Yb^{3+},Eu^{3+} crystals with 0.1 atom % Er^{3+}, the relative intensity

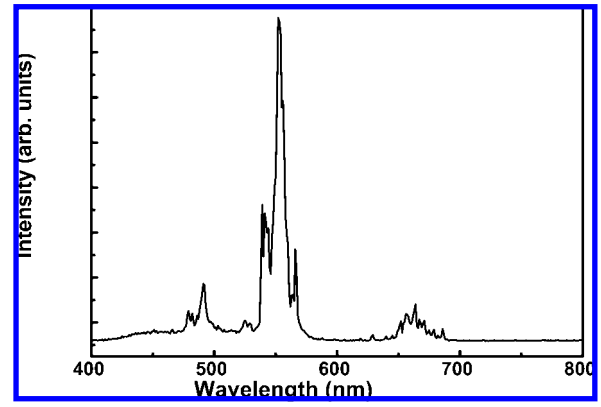

Figure 3. Photoluminescence spectra of Y_2O_3 doped with 2 atom % Yb^{3+} using 970 nm laser diode with power 500 mW.

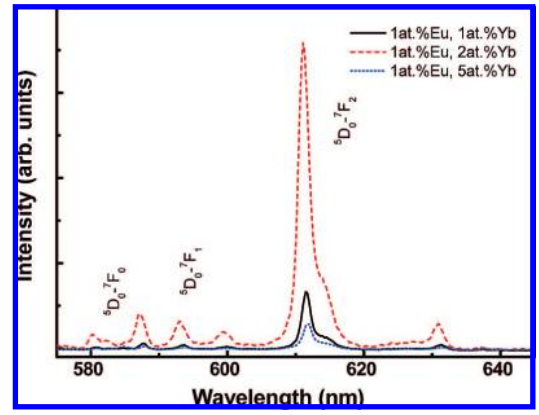

Figure 4. Photoluminescence spectra of Y_2O_3 codoped with 1 atom % Eu^{3+} and various concentrations of Yb^{3+} using a 970 nm laser diode with power 500 mW.

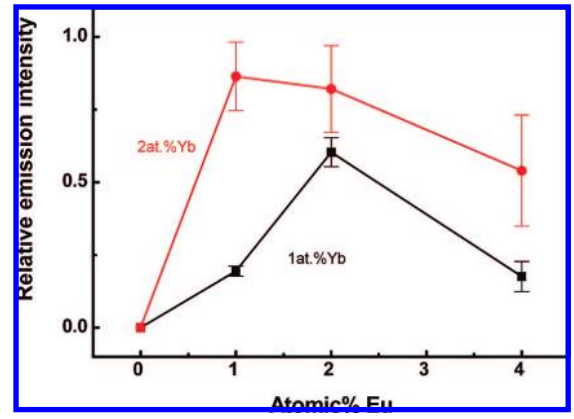

Figure 5. Dependence of the integrated intensity for the $^5D_0 \rightarrow {}^7F_2$ emission transition on Eu^{3+} concentration in Y_2O_3 codoped with 1 or 2 atom % Yb^{3+} using a 970 nm laser diode with power 500 mW. (Values are normalized with respect to the 2 atom % Yb, 1 atom % Eu sample. Results for 3 experiments are shown with standard deviations as error bars).

of Eu^{3+} emission decreased whereas that due to Er^{3+} emission increased considerably. We therefore do not consider that the Er^{3+} impurity plays a role in the Eu^{3+} upconversion process. Figure 5 summarizes the emission intensity trends for samples with 1 and 2 atom % Yb^{3+} doping and for various concentrations of Eu^{3+}. For a nominal doping of Eu^{3+} ion concentration at the constant value of 1 atom %, the sample with 2 atom % Yb^{3+} shows a 4.4-fold higher intensity than that with 1 atom % Yb^{3+}, whereas the intensity for the sample with 5 atom % Yb^{3+} decreases. Samples were also prepared with 2 and 4 atom %

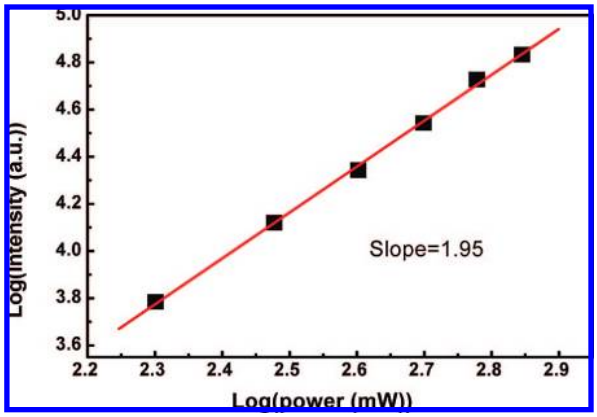

Figure 6. Log−log dependence of $^5D_0 \rightarrow {}^7F_2$ transition intensity upon excitation power.

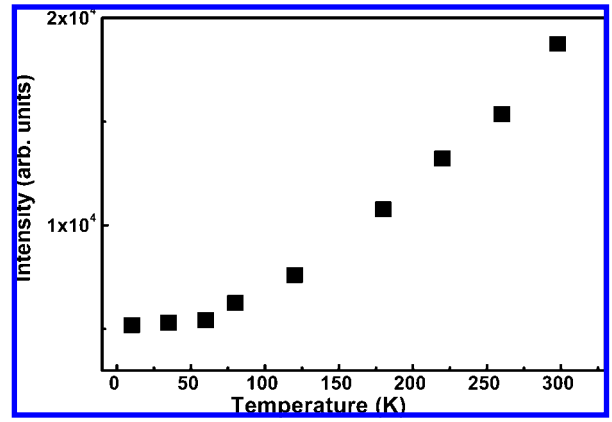

Figure 7. Temperature dependence of the integrated emission intensity at 610 nm for the sample Y_2O_3:1 atom % Eu^{3+}, 2 atom % Yb^{3+}.

Eu^{3+} and varying concentrations of Yb^{3+} (not shown). For the samples with 2 atom % Eu^{3+}, the upconversion emission intensity decreased with the increase of Yb^{3+} concentration from 1 or 2 atom % to 8 atom %. A monotonic decrease in emission intensity was found for the samples doped with 4 atom % Eu^{3+}, when the Yb^{3+} concentration changed from 1 to 2, 4 and 8 atom %. Clearly, factors such as the absorption cross-section and the competition between radiative cooperative emission, energy transfer to Eu^{3+} and energy migration to traps influence the relative emission intensities.

The dependence of the integrated intensity of the Eu^{3+} upconversion emission upon the incident excitation power of laser diode is portrayed in the log−log plot of Figure 6. The slope of the log−log graph is 1.95, which indicates that two photons participate in the cooperative energy transfer process involved with a pair of Yb^{3+} and one Eu^{3+} ion. Several possible two-photon-related mechanisms for cooperative sensitization upconversion luminescence have been given without proofs in previous studies. Clearly, pairs of Yb^{3+} ions are first excited from $^2F_{7/2}$ to $^2F_{5/2}$ upon 970 nm pumping. Either they comprise a (virtual) excited dimer state[30] or two separate Yb^{3+} ions, which deactivate themselves by simultaneously transferring their energy to one nearby Eu^{3+} ion in its ground-state level. Accordingly, the Eu^{3+} ion has been postulated to transit to the $^5D_2$ multiplet term[22] or to the $^5D_1$ multiplet.[20,21] Subsequent nonradiative decay occurs to $^5D_0$, followed by emission.

Some indication of the upconversion mechanism may be deduced from the temperature dependence of the upconversion emission intensity. Figure 7 shows the dependence of the emission intensity of $^5D_0 \rightarrow {}^7F_2$ emission transition (I) upon temperature (T). The graph shows an exponential growth with temperature and may be fitted empirically by:

$$I = (430 \pm 1426) + (4033 \pm 1202)\exp[T/(196.5 \pm 30.1)] \quad (1)$$

4. Discussion

The upconversion process involves de-excitation of two Yb^{3+} ions and excitation of one Eu^{3+} ion (Figure 8). There are many specific mechanisms possible, and it is difficult to discriminate the importance of one against another without resorting to careful consideration and detailed precise calculations. If it is assumed that mechanisms involving short-range exchange interactions are not important, then the part of the effective operator for the excitation of Eu^{3+} ions in the upconversion process can be written as superposition of unitary tensors $U^{(k)}$ ($k = 2, 4, 6$), analogous to the effective electric dipole moment

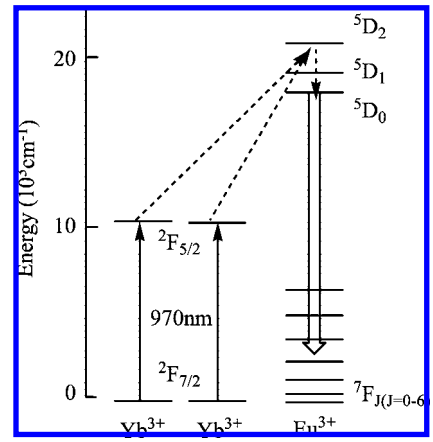

Figure 8. Schematic energy level diagram for Yb^{3+}−Eu^{3+}−Yb^{3+} system for cooperative energy transfer.

operator in Judd−Ofelt theory. The selection rule for $U^{(k)}$ between the initial and final state with angular momentum J_1 and J_2, respectively, is $|J_1 - J_2| \le k \le J_1 + J_2$, that is, the same as the selection rule for $4f^N - 4f^N$ electric dipole transitions. Hence, the upconversion process involving excitation of Eu^{3+} $^7F_0$ to $^5D_{0,1}$, which is only due to J mixing in the states $^7F_0$ and $^5D_{0,1}$, is much weaker than the excitation of Eu^{3+} $^7F_1$ to $^5D_1$, which is directly allowed.

Denoting the energy of the ith crystal field level of Eu^{3+} as E_i and the relative upconversion rate for Eu^{3+} initially in level E_i being A_i, and assuming the Boltzmann distribution for the Eu^{3+} ion, we have the following equations,

$$\Xi(T) = \sum_{i=1}^{N} \exp\left(-\frac{E_i}{k_B T}\right) \quad (2)$$

$$\rho_i(T) = \exp\left(-\frac{E_i}{k_B T}\right)/\Xi(T) \quad (3)$$

$$R(T) = \sum_{i=1}^{N} \rho_i(T) A_i \quad (4)$$

where $\Xi(T)$, $\rho_i(T)$, and $R(T)$ are the distribution function, the probability of occupation of the E_i energy level, and the total upconversion rate, expressed as functions of temperature T. The crystal field energy levels of Eu^{3+} are documented in the literature (in cm^{-1}):[25] (^7F_J) E = [0, 202, 361, 546, 859, 907, 949...]); ($^5D_1$) E = [18 937, 18 961]. The rates A_i are not known, apart from the fact that A_1 is much smaller than others due to

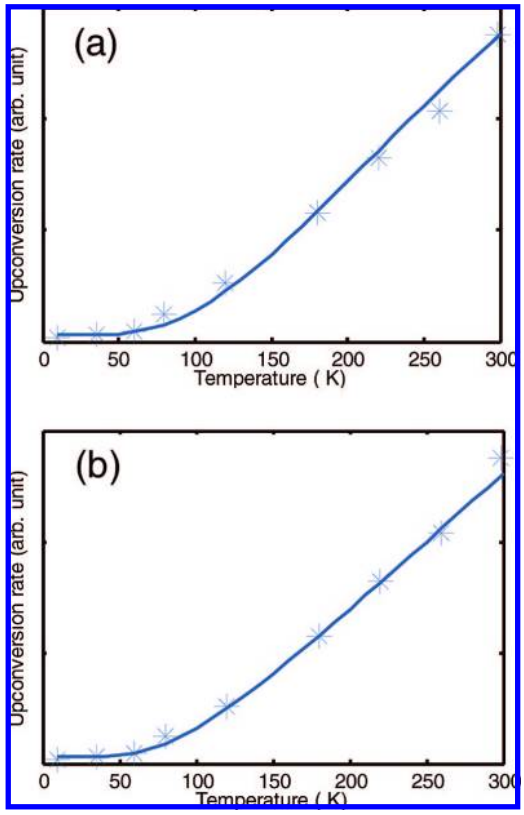

Figure 9. Simulated temperature dependence of the upconversion rate (a) using eqs 2−4 and (b) using eq 5.

the J selection rule and the rates A_4 up to A_N are not important due to their small population distributions at or below room temperature. Because the absolute energy transfer rates cannot be determined in the measurements, the absolute values of these parameters cannot be determined and only the relative values of the parameters make sense. Therefore, one of the parameters is chosen as a unit for reference. Here, we set $A_1 = 1$ and $A_4...A_N = A_3$, and treat A_2 and A_3 as free parameters. A good fit of the measured temperature dependence of the upconversion rate is obtained with $A_2 = 3.8$, $A_3 = 12$ as shown in part a of Figure 9. The reason A_3 turns out to be substantially larger than A_2 may be due to the near resonant nature of the simultaneous process of the de-excitations (expressed in cm^{-1}): 2(Yb^{3+}: 10 225 → 932) and the excitation: Eu^{3+}: 361 → (18 937 or 18 961).

There is an alternative simulation by focusing upon the dependence of the upconversion rates upon temperature. The upconversion process is not usually resonant in electronic energy and thus involves the emission and/or absorption of phonons. Assuming that the dominant process is emission of one phonon of energy $\hbar\omega$, the dependence of the rate on temperature can be written as:

$$A_i(T) = A_i(0)\frac{1}{1-\exp(-\hbar\omega/k_B T)} \qquad (5)$$

Because of the lack of experimental data, we set $A_1(0) = 1$ and assume that all the allowed processes have the same relative rate $A(0)$. Then $A(0)$ and the phonon energy $\hbar\omega$ are treated as fitting parameters. A good fit of experimental data can be obtained with $A(0) = 5$ and $\hbar\omega = 300$ cm^{-1}, as shown in part b of Figure 9. The fitting is not unique because by adjusting simultaneously $A(0)$ in the range 4−6 and $\hbar\omega = 250$ or 400 cm^{-1}, the experimental data can also be fitted quite well.

5. Conclusions

In conclusion, red Eu^{3+} emission has been observed from infrared laser diode excitation of Y_2O_3:Eu^{3+},Yb^{3+}. Because the Y_2O_3:Yb^{3+} absorption band is fairly wide, the possibility of broadband excitation exists. For the Eu^{3+} concentration of 1 atom %, the optimum Yb^{3+} concentration is 2 atom %. The upconversion rate shows an increase with increasing temperature, and the main reason is the thermal excitation of Eu^{3+} to $^7F_1$ levels with higher upconversion rate. The temperature dependence of the upconversion rate has been satisfactorily simulated.

Acknowledgment. This work is supported by the Hong Kong RGC Competitive Earmarked Research Grant CityU 102607.

References and Notes

(1) Pollnau, M.; Gamelin, D. R.; Lüthi, S. R.; Güdel, H. U.; Hehlen, M. P. *Phys. Rev. B* **2000**, *61*, 3337.
(2) Gamelin, D. R.; Güdel, H. U. *Top. Curr. Chem.* **2001**, *214*, 1.
(3) Auzel, F. *J. Lumin.* **1990**, *45*, 341.
(4) Chen, X.; Song, Z. *J. Opt. Soc. Am.* **2007**, *24*, 965.
(5) Zhang, J.; Wang, S.; Rong, T.; Chen, L. *J. Am. Ceram. Soc.* **2004**, *87*, 1072.
(6) Song, H.; Sun, B.; Wang, T.; Lu, S.; Yang, L.; Chen, B.; Wang, X.; Kong, X. *Solid State Commun.* **2004**, *132*, 409.
(7) Vetrone, F.; Boyer, J.-C.; Capobianco, J. A.; Speghini, A.; Bettinelli, M. *J. Appl. Phys.* **2004**, *96*, 661.
(8) Auzel, F. *C. R. Hebd. Seances Acad. Sci.* **1966**, *262*, 1016.
(9) Auzel, F. *C. R. Hebd. Seances Acad. Sci.* **1966**, *263*, 819.
(10) Miyakawa, T.; Dexter, D. L. *Phys. Rev. B* **1970**, *1*, 70.
(11) Fong, F. K.; Diestler, D. J. *J. Chem. Phys.* **1972**, *56*, 2875.
(12) Kushida, T. *J. Phys. Soc. Jpn.* **1973**, *34*, 1327.
(13) Chua, M.; Tanner, P. A. *J. Lumin.* **1996**, *66&67*, 203.
(14) Salley, G. M.; Valiente, R.; Guedel, H. U. *J. Lumin.* **2001**, *94−95*, 305.
(15) Salley, G. M.; Valiente, R.; Güdel, H. *Phys. Rev. B* **2003**, *67*, 134111.
(16) Valiente, R.; Wenger, O.; Güdel, H. *Chem. Phys. Lett.* **2000**, *320*, 639.
(17) Reinhard, C.; Gerner, P.; Valiente, R.; Wenger, O. S.; Güdel, H. U. *J. Lumin.* **2001**, *94−95*, 331.
(18) Tanner, P. A.; Wong, K.-L. *J. Phys. Chem. B* **2004**, *108*, 136.
(19) Laversenne, L.; Guyot, Y.; Goutaudier, C.; Cohen-Addad, M. Th.; Boulon, G. *Opt. Mater* **2001**, *16*, 475.
(20) Dwivedi, Y.; Thakur, S. N.; Rai, S. B. *Appl. Phys. B: Laser Opt.* **2007**, *89*, 45.
(21) Maciel, G. S.; Biswas, A.; Prasad, P. N. *Opt. Commun.* **2000**, *178*, 65.
(22) Jubera, V.; Garcia, A.; Chaminade, J. P.; Guillen, F.; Sablayrolles, J.; Fouassier, C. *J. Lumin.* **2007**, *124*, 10.
(23) Yamada, N.; Shionoya, S.; Kushida, T. *J. Phys. Soc. Jpn.* **1972**, *32*, 1577.
(24) Yuan, J.-L.; Zeng, X.-Y.; Zhao, J.-T.; Zhang, Z.-J.; Chen, H.-H.; Yang, X.-X. *J. Phys. D: Appl. Phys* **2008**, *41*, 105406.
(25) Morrison, C. A.; Leavitt, R. P. *Handbook on the Physics and Chemistry of Rare Earths*; Gschneidner, K. A., Eyring, L., Eds.; North-Holland: Amsterdam, 1982; p 567.
(26) Lupei, A.; Lupei, V.; Enaki, V. N.; Presura, C.; Petraru, A. *Spectrochim. Acta A* **1999**, *55*, 773.
(27) Louis, C.; Bazzi, R.; Flores, M. A.; Zheng, W.; Lebbou, K.; Tillement, O.; Mercier, B.; Dujardin, C.; Perriat, P. *J. Solid State Chem.* **2003**, *173*, 335.
(28) Mercier, B.; Dujardin, C.; Ledoux, G.; Louis, C.; Tillement, O.; Perriat, P. *J. Lumin.* **2006**, *119−120*, 224.
(29) Dou, C. G.; Yang, Q. H.; Hu, X. M.; Xu, J. *Opt. Commun.* **2008**, *281*, 692.
(30) Hehlen, M. P.; Güdel, H. U. *J. Chem. Phys.* **1993**, *98*, 1768.

JP8046505